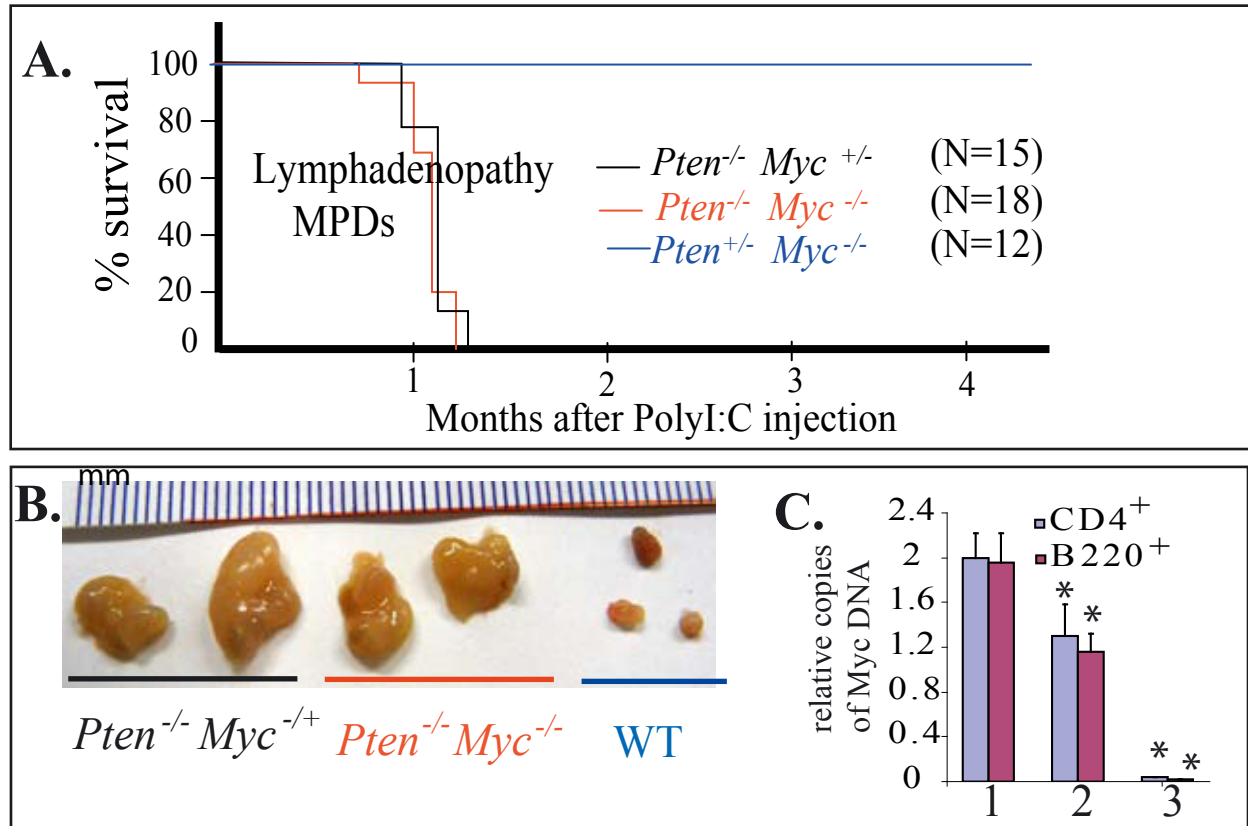
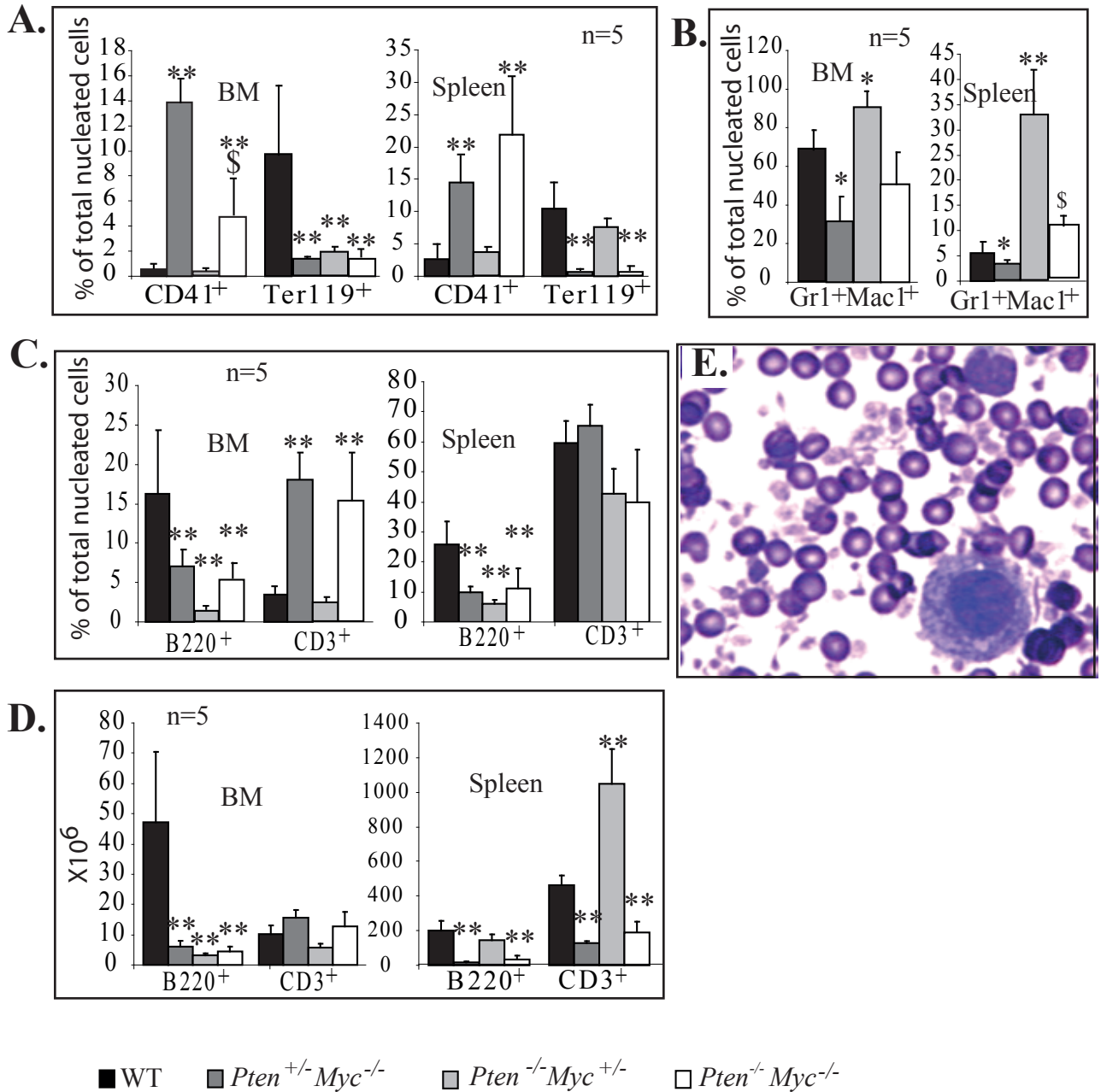


Supplementary Data 1. Lymphocytes isolated from $Cre^+Pten^{fx/fx}/Myc^{fx/fx}$ LPDs mice failed to engraft to hematopoietic tissues in recipient mice, whereas lymphoblasts from $Cre^+Pten^{fx/fx}/Myc^{fx/+}$ mice with lymphoma generated a leukemia-like disease with lymphoblast infiltration into multiple tissues. Lymphocytes and lymphoblasts were isolated from the enlarged lymph nodes of $Cre^+Pten^{fx/fx}/Myc^{fx/fx}$ mice with LPDs and $Cre^+Pten^{fx/fx}/Myc^{fx/+}$ mice with lymphoma. Cells were transplanted into lethally- irradiated recipient mice separately. Ten million $Cre^+Pten^{fx/fx}/Myc^{fx/fx}$ LPD lymphocytes (CD45.2⁺) or one million $Cre^+Pten^{fx/fx}/Myc^{fx/+}$ lymphoblasts (CD45.2⁺) were transplanted into each recipient mouse together with 2×10^5 WT supporting BM cells (CD45.1⁺). Eight mice were transplanted in each group. Mice receiving $Cre^+Pten^{fx/fx}/Myc^{fx/fx}$ LPD lymphocytes survived for more than 6 months. No donor- derived cells (CD45.2⁺) could be detected in BM (A) and spleens (B) of recipient mice 6 months after transplantation, as shown by flow cytometric analysis of CD45.2⁺ cells. However, all mice receiving $Cre^+Pten^{fx/fx}/Myc^{fx/+}$ lymphoblasts died within 20 days after transplantation with a leukemia-like disease as shown by multiple tissue infiltration of CD4⁺CD8⁻ lymphoblasts (C-F). C and D are representative flow data from BM (C) and spleen (D) of one such recipient mouse. F. A representative liver section shows lymphoblast infiltration of the liver tissue.



Supplementary Data 2. A & B. Three weeks after birth, $Mx1Cre^+ Pten^{fx/fx} Myc^{fx/fx}$, $Mx1Cre^+ Pten^{fx/fx} Myc^{fx/+}$, $Mx1Cre^+ Pten^{fx/+} Myc^{fx/fx}$, and WT littermate control mice were injected with 200ug. polyI:C every other day for a total of 5 injections to induce gene deletions. All $Mx1Cre^+ Pten^{fx/fx} Myc^{fx/fx}$ and $Mx1Cre^+ Pten^{fx/fx} Myc^{fx/+}$ mice developed lymphadenopathy 20 to 30 days after *Pten* and *Myc* gene deletions were induced. **C.** Heterozygous or homozygous *Myc* deletion in CD4⁺ and B220⁺ lymphocytes isolated from enlarged lymph nodes were confirmed by q-PCR assay. 1, 2 and 3 represent CD4⁺ or B220⁺ cells isolated from WT lymph nodes, $Mx1Cre^+ Pten^{fx/fx} Myc^{fx/+}$ lymphadenopathy and $Mx1Cre^+ Pten^{fx/fx} Myc^{fx/fx}$ lymphadenopathic mice, respectively

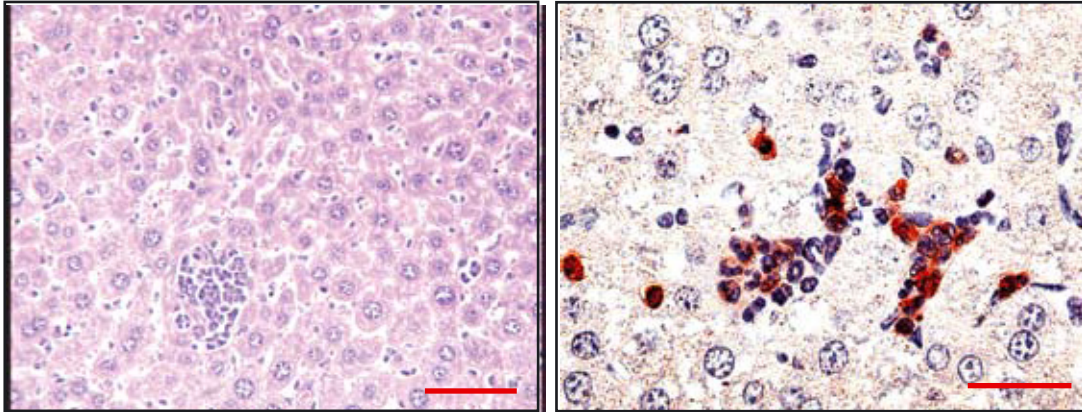


Supplementary Data 3: General hematopoietic information for *Pten*^{-/-}*Myc*^{-/-} mice.

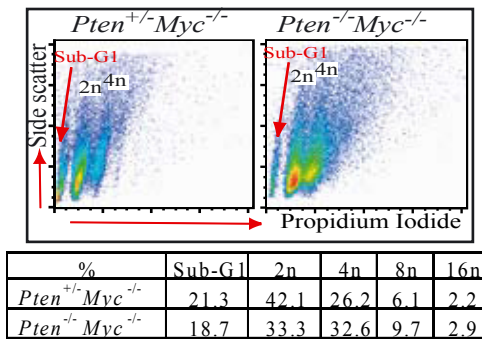
A.

Reduction in the percentage of CD41⁺ megakaryocytes in BM but increased percentage of these same cells in spleens of *Pten*^{-/-}*Myc*^{-/-} mice compared to *Pten*^{+/-}*Myc*^{-/-} mice. **B.** Slight increase in the percentage of Gr1⁺Mac1⁺ granulocytes in spleens of *Pten*^{-/-}*Myc*^{-/-} mice compared to those of *Pten*^{+/-}*Myc*^{-/-} mice. **C.** Significant reduction in B220⁺ B lymphocytes in BM and spleens of *Pten*^{-/-}*Myc*^{-/-} and *Pten*^{+/-}*Myc*^{-/-} mice. However the percentage of CD3⁺ T-lymphocytes is significantly increased in BM but remains the same in spleens of *Pten*^{-/-}*Myc*^{-/-} and *Pten*^{+/-}*Myc*^{-/-} mice compared to WT control mice. The percentages of these two types of cells are comparable between *Pten*^{-/-}*Myc*^{-/-} and *Pten*^{+/-}*Myc*^{-/-} mice. **D.** Absolute numbers of B220⁺ B-lymphocytes and CD3⁺ T-lymphocytes are comparable between *Pten*^{-/-}*Myc*^{-/-} and *Pten*^{+/-}*Myc*^{-/-} mice. **E.** A few megakaryocytes are occasionally observed in the PB of *Pten*^{-/-}*Myc*^{-/-} mice. ** indicates statistical significance compared to WT mice. \$ indicates statistical significance compared to *Pten*^{-/-}*Myc*^{+/-} mice.

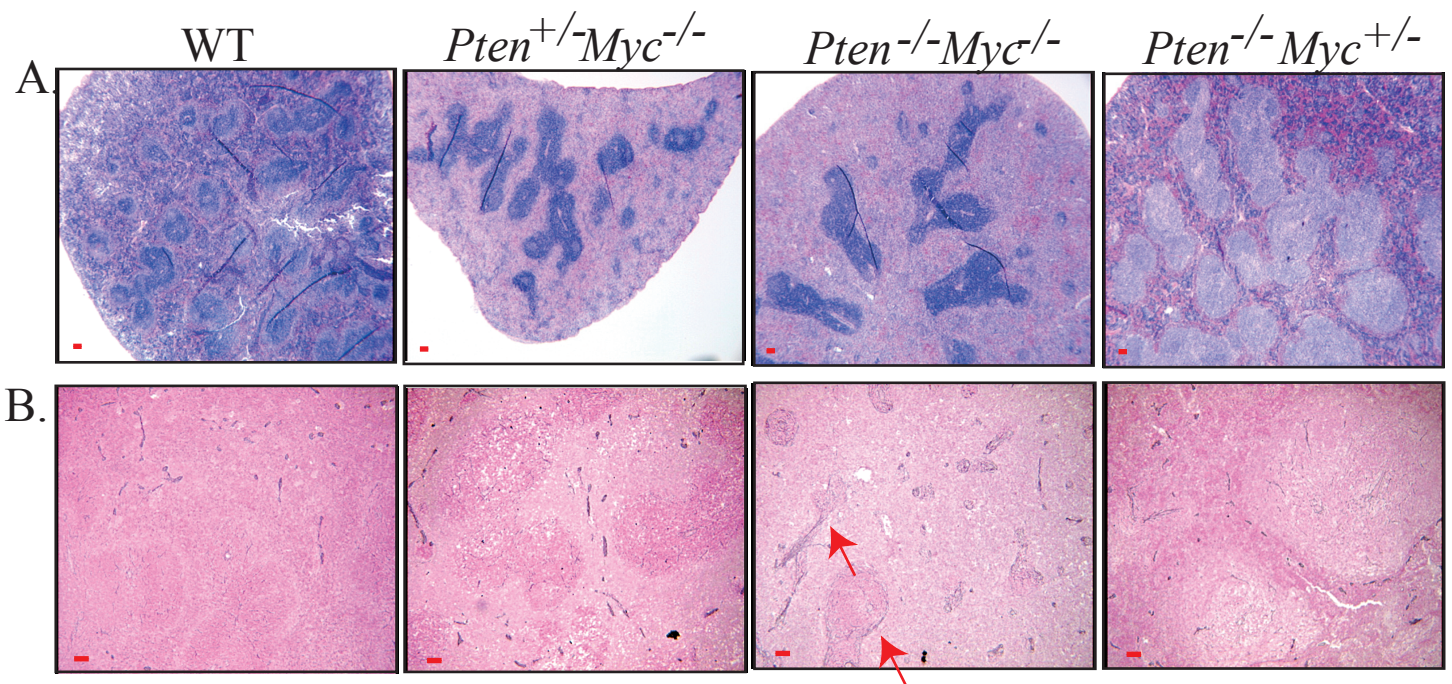
Pten^{-/-}*Myc*^{+/-}



Supplementary data 4. Granulocyte infiltration into livers of *Pten*^{-/-}*Myc*^{+/-} mice, as shown by Gr1 antibody staining. Bars in the figures equal 100 μ m.



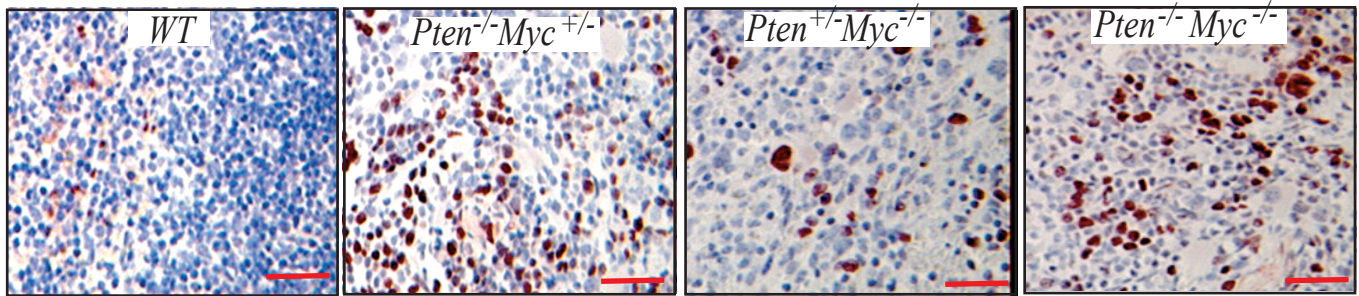
Supplementary Data 5. *Pten* deletion did not reverse the lower ploidy and increased apoptosis phenotype of *Myc*^{-/-} megakaryocytes. PI staining and flow cytometric analysis of DNA content of CD41⁺ megakaryocytes from *Pten*^{+/-}*Myc*^{-/-} and *Pten*^{-/-}*Myc*^{-/-} mice. Upper panel is representative flow cytometric data for three pairs of mouse analyses. The sub-G1 population consists of cells undergoing apoptosis.



Supplementary Data 6. Increased fibrosis in the spleens of *Pten*^{-/-}*Myc*^{-/-} mice.

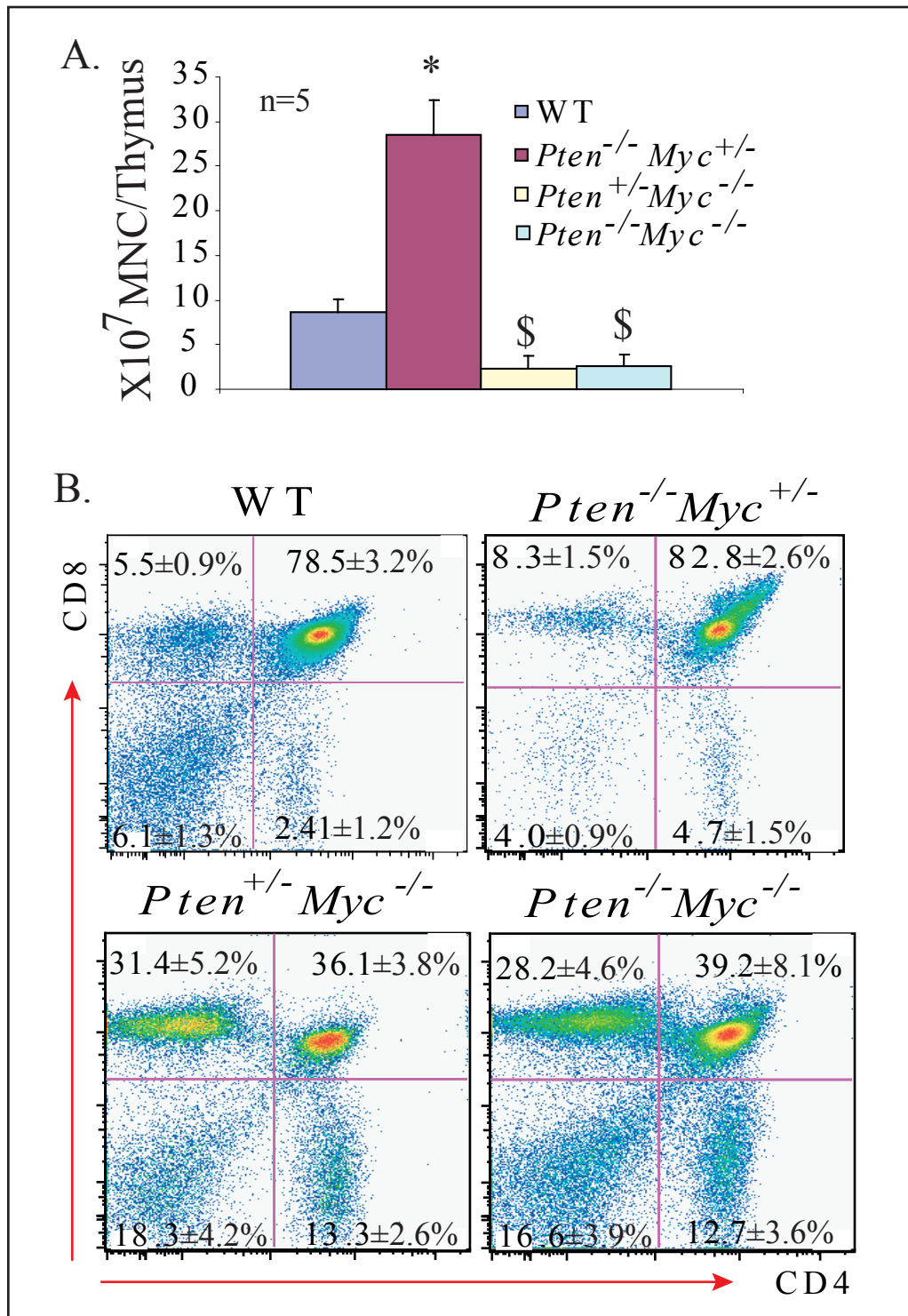
A & B.

Spleen sections of WT, *Pten*^{+/-}*Myc*^{-/-}, *Pten*^{-/-}*Myc*^{-/-} and *Pten*^{+/-}*Myc*^{-/-} mice stained with H & E (A) and reticulin (B). Increased fibrosis in *Pten*^{-/-}*Myc*^{-/-} mouse spleen is indicated by with arrows (B). Bars in the figures equal 100µm.



Supplementary Data 7. Increased megakaryocytic proliferation in *Pten*^{-/-}*Myc*^{-/-} mice.

Representative images of *in situ* BrdU staining of spleen sections from WT, *Pten*^{-/-}*Myc*^{+/-}, *Pten*^{+/-}*Myc*^{-/-} and *Pten*^{-/-}*Myc*^{-/-} mice. Significantly increased BrdU⁺ cell percentage in spleens of *Pten*^{-/-}*Myc*^{+/-} and *Pten*^{-/-}*Myc*^{-/-} mice. The BrdU⁺ cells in *Pten*^{+/-}*Myc*^{-/-} and *Pten*^{-/-}*Myc*^{-/-} mice are relatively larger in size, suggesting that they are megakaryocytes.



Supplementary Data 8. Reduction of thymocyte numbers in thymus glands of *Pten*^{+/-}*Myc*^{-/-} and *Pten*^{-/-}*Myc*^{-/-} mice. **A.** Total mononucleated cell numbers (MNCs) in thymus glands of WT, *Pten*^{-/-}*Myc*^{+/-}, *Pten*^{+/-}*Myc*^{-/-} and *Pten*^{-/-}*Myc*^{-/-} mice. **B.** CD4 and CD8 staining and flow cytometric analysis of thymocytes in the thymuses of mutant mice.